Experimental and Thermodynamic Modeling of CO_2 Absorption into Aqueous DEA and DEA+Pz Blended Solutions

Kazemi, Shima
Department of Applied Chemistry, North Tehran Branch, Islamic Azad University, Tehran, I.R. IRAN

Ghemi, Ahad*[+]
School of Chemical, Petroleum and Gas Engineering, Iran University of Science and Technology, Tehran, I.R. IRAN

Tahvildari, Kambiz
Department of Applied Chemistry, North Tehran Branch, Islamic Azad University, Tehran, I.R. IRAN

ABSTRACT: *The important environmental concern of the carbon dioxide (CO_2) capture by the absorption process with amine solutions is studied in the current study. The experiments are performed at operating conditions of a temperature range of 25–65 ℃, a pressure range of 1.5–6.5 bar, diethanolamine (DEA) concentration of 0– 1.5 M, PZ concentration of 0– 0.5 M, and stirrer speed of 0–300 rpm. The effects of operating conditions on CO_2 loading, absorption rate, and mass transfer flux are investigated into two solutions of DEA and DEA+piperazine (Pz) blend in a stirred reactor. In the DEA+CO_2+H_2O system, by increasing stirrer speed from 0 to 300 rpm, the maximum values of CO_2 loading and mass transfer flux at the same DEA concentration are increased 65% and 137%, respectively. The CO_2 loading and mass transfer flux have higher values at higher initial pressures. The predicted values for species concentrations into the DEA+CO_2+H_2O system are also evaluated based on the Pitzer model, mass, and charge balance equations. The results showed that by increasing stirrer speed, the concentration of DEA molecule is decreased 40% but the concentrations of other ions and molecules are increased. In the DEA+Pz+CO_2+H_2O system, the results indicated that adding Pz to the absorbent solution was more efficient in CO_2 capture relative to only the DEA solution. The equilibrium CO_2 loading is increased by 20% and 16% for blend solutions with 4:6 and 6:4 molar ratios of DEA and Pz, respectively, but using only Pz solution is increased it up to 29%.*

KEYWORDS: *CO_2 absorption; DEA; Pz; Blended amine; Mass transfer flux; Thermodynamic.*

INTRODUCTION

The anthropogenic carbon dioxide (CO_2) emissions as a global environmental concern have caused greenhouse problems and acid rain phenomenon that have attracted the attention of several researchers and industrialists [1].

***** *To whom correspondence should be addressed.*
+ *E-mail: aghaemi@iust.ac.ir*
1021-9986/2021/4/1162-1178 17/$/6.07

The application of amine solutions to capture CO_2 from process gas streams is a chemical absorption method and a good viable option [2]. The chemical absorption process is more economical than other processes such as cryogenic distillation, membrane separation, and adsorption [3-6]. The conventional amines used in these processes are monoethanolamine (MEA), diethanolamine (DEA), methyl-diethanolamine (MDEA), and 2-amino-2-methyl-1-propanol (AMP) [7]. But only using these amines is not very efficient to absorb CO_2 because of their problems such as equipment corrosively, foaming tendency, low absorption capacity, and rate. Several experimental [8-10] and modeling [11-13] studies have been performed to screen solvent and investigate the properties of amine solutions such as absorption capacity, reaction kinetics, and regenerative potential. Based on these studies, the single aqueous amine solutions have been executed well in some desired CO_2 capture applications, but several disadvantages were also observed such as the limitation of CO_2 capture capacity and high regeneration energy consumption [14,15].

The mixed solvents have been proposed to enhance CO_2 capture performance, but the solvent stability reduces by blending one amine with other amines [16,17]. Therefore, the absorption rate can be improved by adding activators such as piperazine (Pz) to these amines because of their high reaction rate with CO_2 [18-22]. Pz is a cyclic diamine with two secondary amino groups used as an efficient promoter for the absorption rate. The aqueous Pz solution has a higher absorption rate and capacity than the other activators [23-24]. The Pz-based amine blends could diminish the precipitation problems of concentrated Pz, while maintaining the high CO_2 capacity and rate [25-27].

The measurement of the equilibrium CO_2 loading capacity in the absorption processes is one of the most important variables to assess the absorbent efficiency and separation rate [28]. In recent years, several researchers have been developed thermodynamic models to evaluate the equilibrium CO_2 solubility under various conditions and solutions [29]. *Zhu et al*. [30] used the Pz solution in the CO_2 absorption process and their results showed that the reaction between CO_2 and Pz had the second-order kinetic rate constant with a magnitude order higher than one for the pure MEA solvent.

Ramazani et al. [31] measured the equilibrium CO_2 solubility in a MEA+PZEA aqueous solution experimentally using the vapor-liquid equilibrium equipment. Based on Response Surface Methodology (RSM) and analysis of variance (ANOVA), an acceptable agreement was shown between the statistical model and experimental data. Also, the maximum CO_2 loading capacity was obtained by optimization of the molar ratio of PZEA to MEA.

Nwaoha et al. [32] carried out experiments using a highly concentrated tri-solvent blend including AMP, Pz, and MEA to investigate its potential capacity. It has been found that by optimization of the molar ratio of AMP to PZ in the blend, the heat duty was reduced significantly.

Hairul et al. [33] developed a new steady-state model based on the rate into a PZ+AMP solution in a packed column. They considered several parameters such as column hydraulic, mass transfer resistance, and chemical reaction in their model and simulate the absorption process under various CO_2 partial pressures. Based on their results, the model requires a correction for the mass transfer coefficient to predict the profile of CO_2 concentration along the column.

Wang et al. [34] studied an amine solution with a blend of two promising diamines, Pz, N-(2-aminoethyl) ethanolamine (AEEA) in a wetted wall column to modify CO_2 absorption. From their simulation results in terms of molecular geometry deformation and activation energy, the Pz chooses a direct reaction with the CO_2 rather than the reaction with the AEEA-CO_2.

Du et al. [35] analyzed 36 novel Pz-based amine blends for CO_2 capture based on their thermal stabilities. By surveying the degradation mechanism, a relationship between structure and thermal stabilities of the blended amines was found. *Das et al*. [36] utilized a novel aqueous solution of bis (3-aminopropyl) amine (APA) to increase enhancement factors relative to aqueous MDEA solution for CO_2 capture. It has resulted that the second-order rate constant and reaction rate with CO_2 was higher than Pz and 2-(1-piperazine) - ethylamine (PzEA), etc. based on nuclear magnetic resonance spectroscopy method.

Zhang et al. [37] investigated the mass transfer performance for an aqueous blended solution by a combination of N, N-dimethylethanolamine (DMEA), and monoethanolamine (MEA) in a hollow fiber membrane contactor. They examined the effects of various operating conditions such as liquid velocity, inlet gas flow rate, CO_2 partial pressure, feed temperature range, CO_2 lean loading,

amine concentration, and membrane contactor height on the overall mass transfer coefficient and CO_2 flux. In addition, they developed a new correlation to predict the overall gas-phase mass transfer coefficient with an average relative error lower than 10%. *Zhang et al*. [38] also examined the reactions of CO_2 absorption in binary amine solvents (the binary mixtures of MEA/Pz/AMP/DEA). Their results indicated that the Pz had a significant impact on MEA/DEA/AMP in the interactive reactions.

Saidi [39] developed a rate-based mathematical model using an aqueous MDEA+Pz blended solution in a Hollow Fiber Nembrane Contactor (HFMC). Their outcomes expressed that adding Pz to MDEA solution had significant impacts on the CO_2 capture efficiency and the reaction rate was very higher than tri-ethanolamine (TEA) and MDEA solutions.

Suleman et al. [40] performed an experimental and modeling study to measure the CO_2 solubility in the two separated aqueous blends of AMP+MDEA and Pz+MDEA in the high gas loading region. They correlated experimental solubilities for both solutions by a hybrid Kent-Eisenberg model accurately. *Afkhamipour et al*. [41] evaluated the equilibrium behavior of DEAE+Pz solutions by the Deshmukh-Mather (D-M) thermodynamic model. They obtained the excess properties such as Gibbs energy, heat capacity, and enthalpy as a function of CO_2 loading and also predicted the pH and activity coefficient of the solution.

The results of the literature review indicate that the use of mixed amines is used to increase the absorption loading and reaction rate in CO_2 absorption processes [42-44]. In the previous works thermodynamic and the effect of operating conditions on mixed amine loading and mass transfer rate were not considered. In the current study, the CO_2 absorption into the DEA and DEA+Pz blend solutions in a stirred reactor is studied experimentally. The thermodynamic of the DEA+H_2O+CO_2 system was modeled using the Pitzer model with presenting ionic and molecular components of the system. In addition, the effect of operating conditions including stirrer speed, time, amine concentration, temperature, and pressure on CO_2 loading and mass transfer were investigated.

THEORETICAL SECTION

Kinetics and mechanism

The main reactions between CO_2 and individual primary/secondary amines can be described by two steps; zwitterion formation and intermolecular hydrogen transfer mechanisms. In the first step, the CO_2 molecule reacts with one amine molecule but in the second step, one CO_2 molecule reacts with two amine molecules. The equations of CO_2 reactions in the chemical absorption process into the aqueous solution of DEA+Pz blend system are given below [37, 38]:

Piperazine protonation:

$$PZ + H^+ \Leftrightarrow PZH^+ \quad (1)$$

$$PZH^+ + H^+ \Leftrightarrow PZH_2^{2+} \quad (2)$$

Piperazine carbamate formation:

$$PZ + HCO_3^- \Leftrightarrow PZCOO^- + H_2O \quad (3)$$

Piperazine di-carbamate formation:

$$PZCOO^- + HCO_3^- \Leftrightarrow PZ(COO^-)_2 + H_2O \quad (4)$$

Protonated piperazine carbamate formation:

$$PZCOO^- + H^+ \Leftrightarrow PZH^+COO^- \quad (5)$$

Zwitterion formation:

$$DEA + CO_2 \Leftrightarrow DEA^+COO^- \quad (6)$$

$$PZ + CO_2 \Leftrightarrow PZ^+COO^- \quad (7)$$

Intermolecular hydrogen transfer:

$$PZ^+COO^- + PZ \Leftrightarrow PZCOO^- + PZH^+ \quad (8)$$

$$PZ^+COO^- + DEA \Leftrightarrow PZCOO^- + DEAH^+ \quad (9)$$

$$DEA^+COO^- + DEA \Leftrightarrow DEACOO^- + DEAH^+ \quad (10)$$

$$DEA^+COO^- + PZ \Leftrightarrow DEACOO^- + PZH^+ \quad (11)$$

Carbamate and bicarbonate formations and water ionization also occur in the process that their equations are shown in the thermodynamic modeling section.

Mass transfer models

In the CO_2 absorption process, the CO_2 is removed from the gas phase into the liquid phase (absorbent) by transferring across the interface between the phases. The CO_2 absorption flux can be computed from [45]:

$$N_{CO_2} = \frac{\dot{n}}{V \times a} = k_1 (C^t_{CO_2,int} - C^t_{CO_2,b}) \times E \quad (12)$$

Where N_{CO2} is the mass transfer flux of CO_2, k_l is the physical liquid-side mass transfer coefficient [46], $C^t_{CO2,i}$ and $C^t_{CO2,b}$ are the total free concentration of CO_2 at the interface and the liquid bulk, respectively. E is the enhancement factor, which is calculated as the liquid side mass transfer ratio does not stay the same time at the phase interface surface.

Film parameter

The film parameter is a significant parameter that distinguishes how the chemical reactions influenced the mass transfer rate. This parameter is known by the Hatta number defined as the ratio of the maximum amount of consumed component in the liquid film and the maximum amount transferred if no chemical reaction occurs and at zero bulk concentration. It should be noted that all CO_2 reactions should be considered to calculate the film parameter [47]. The dimensionless Hatta number is defined as follows:

$$Ha^2 = \frac{K_{app} \times D_{CO_2-Absorbent}}{k_l^2} \quad (13)$$

Where k_{app} is the apparent reaction rate constant, $D_{CO2\text{-}PZ\text{-}DEA}$ is the CO_2 diffusion coefficient into the Pz+DEA blend solution and k_l is the liquid mass transfer coefficient [48].

Surface renewal theory

According to this theory, the liquid elements do not stay at the same time at the phase interface [49]. The mass transfer flux based on this theory can be defined as follows:

$$N_{CO_2} = E k_l (C_{CO_{2,int}} - C_{CO_{2,b}}) \quad (14)$$

The mass transfer flux coupled with chemical reactions is described as:

$$N_{CO_2} = k_l \sqrt{1+M} (C_{CO_{2,int}} - C_{CO_{2,b}}) = \quad (15)$$

$$\sqrt{k_l^2 + k_{app} D_{CO_2-absoebent}} (C_{CO_{2,int}} - C_{CO_{2,b}})$$

The enhancement factor in the surface renewal theory is determined by:

$$E = \frac{N_{CO_2}}{k_l (C_{CO_{2,int}} - C_{CO_{2,b}})} = \quad (16)$$

$$\frac{k_l \sqrt{1+M} (C_{CO_{2,int}} - C_{CO_{2,b}})}{k_l (C_{CO_{2,int}} - C_{CO_{2,b}})} = \sqrt{1+M}$$

Mass transfer coefficient can be depicted by series resistances. The overall resistance relation in the physical absorption based on this theory is presented below [49].

$$\frac{1}{k_G} = \frac{1}{k_g} + \frac{H_{CO_2,H_2O}}{E k_l} \quad (17)$$

Based on Eqs. (16) and (17):

$$\frac{1}{k_G} = \frac{1}{k_g} + \frac{H_{CO_2,H_2O}}{\sqrt{k_l^2 + k_{app} D_{CO_2-absorbent}}} \quad (18)$$

And:

$$k_l' = \frac{\sqrt{k_l^2 + k_{app} D_{CO_2-absorbent}}}{H_{CO_2,H_2O}} = \frac{k_l \sqrt{1+M}}{H_{CO_2,H_2O}} \quad (19)$$

Where M is the film parameter is defined in the following:

$$M = \left(\frac{k_l' \times H_{CO_2,H_2O}}{k_l}\right)^2 - 1 \quad (20)$$

EXPERIMENTAL SECTION

Materials and methods

The aqueous diethanolamine (DEA) solution, i.e. the first absorbent was prepared from Merck Switzerland with a high purity greater than 99%. To make the blend solution, the piperazine as the second absorbent was mixed with DEA at different concentrations. A mixture of CO_2 and air as the gas phase flow with a purity of 99.99% was used which was supplied by the Hamtagas Mehrabad Co. cylinder. Double distilled water was utilized to prepare the two desirable solutions.

Experimental setup

A schematic view of the experimental setup of the CO_2 absorption process used in the present study is shown in Fig. 1. The required amount of CO_2 was supplied by a gas cylinder heated by a heater. The pressure and temperature were measured by a pressure sensor and calibrated thermocouple, respectively. A stirrer was used in a batch reactor to change stirrer speed during the processing time. The CO_2 enters the reactor inlet that its rate was set by the inlet valve and discharge from the reactor outlet. It should be noted that the pure CO_2 gas was sent to the reactor cell to eliminate the existing air. When the temperature was adjusted,

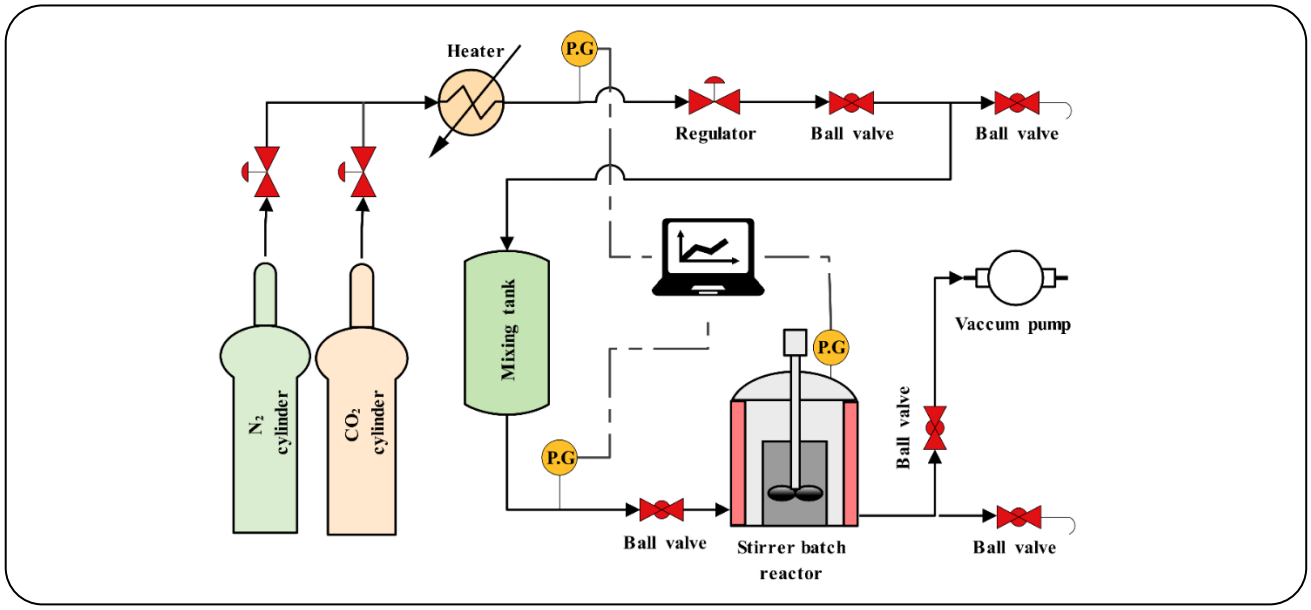

Fig. 1: Schematic view of the experimental setup.

the gas has entered a cell containing the desired absorbent placed inside the reactor and the stirrer turned on and at this time the absorption process started until the equilibrium state of the process. The equilibrium state of the CO_2 absorption process is obtained when the variation of the pressure tends to zero which this state occurred after one hour in this study. As time elapses, the CO_2 pressure reduces due to absorption by the solvent. The stirrer speed was varied to investigate its effects on the amount of absorbed CO_2. The absorbent volume in all experimental tests was 20 mL. The temperature and pressure of the process were recorded at each time step to calculate the CO_2 loading.

Experimental measurement

The CO_2 concentration was measured using the gas analyzer and the absorption rate was calculated by the material balance of the gas phase. The CO_2 absorption rate into the DEA-Pz solution is determined from the experimental data as follows:

$$\text{Absorption rate}\ (\%) = \frac{P_{i0} - P_f}{P_i} \times 100 \tag{21}$$

Where P_i and P_f are the initial and final pressures of the stirrer reactor, respectively [50]. The CO_2 loading (α) is referred to the number of absorbed CO_2 moles relative to the number of absorbent moles as below equation:

$$\alpha = \frac{n_{CO_2}}{\sum n_{solvent}} \tag{22}$$

Where n_{CO2} is the mole of absorbed CO_2 at each time and $n_{solvent}$ is the sum of amine moles and another absorbent in the blend solution [51].

THERMODYNAMIC MODELING OF DEA SOLUTION

Kinetics

In the present study, species concentrations in the liquid bulk are modeled and predicted for a single DEA solution. The reactions into the aqueous DEA solution are as follow [52]:

Dissociation of the protonated amine:

$$DEAH^+ \xleftarrow{K_1} DEA + H^+ \tag{23}$$

Formation of carbamate:

$$DEACOO^- + H_2O \xleftarrow{K_2} DEA + HCO_3^- \tag{24}$$

Dissociation of CO_2:

$$CO_2 + H_2O \xleftarrow{K_3} HCO_3^- + H^+ \tag{25}$$

Dissociation of bicarbonate ion:

$$HCO_3^- \xleftarrow{K_4} CO_3^{2-} + H^+ \tag{26}$$

Ionization of water:

Table 1: The constant of equilibrium constant as a function of temperature

K	a	b	c	d× 10^2	e × 10^{-5}	Temperature (K)	Reference
$\ln(K_i)=\frac{a_i}{T}+b_i\ln(T)+c_i\times T+d_i$							
K_1	-3071.15	6.776904	0	-4878.94	-	273.15-353.15	[54]
K_2	-17067.2	-66.8007	0	43970.9	-	303.15-358.15	[53]
$H_{CO2,H2O}$	-6789.04	-11.4519	-0.010454	9449.14	-	273.15- 498.15	[55]
$\ln(K_i)=a_i+\frac{b_i}{T}+c_i\ln(T)+d_i\times T+\frac{e_i}{T^2}$							
K_3	1203.1	68359.6	188.444	-20.6428	-47.1291	273.15-673.15	[56]
K_4	175.36	-7230.6	-30.509	1.31478	-3.72805	273.15-523.15	[57]
K_5	140.932	-13446	-22.48	0	0	273.15-498.15	[58]

$$H_2O \xleftarrow{K_5} OH^- + H^+ \quad (27)$$

Where K_i is the equilibrium constant, which can be correlated as a function of temperature represented in Table 1. The concentration of the CO_2 in the liquid phase can be predicted by Henry's law as follows [53]:

$$P_{CO_2} = H_{CO_2} \times C_{CO_2} \quad (28)$$

The equilibrium constant of chemical reactions

The chemical equilibrium constant is defined as below equation[59]:

$$K = \prod_i (m_i \gamma_i)^{\nu_i} \quad (29)$$

Where m_i, γ_i and ν_i are the molality, activity coefficient and stoichiometric coefficient of component i into the solution are respectively. All chemical equilibrium constants are stated in the molality scale specified mathematically as follow [52]:

$$K_1 = \frac{\left[H^+\right]_{eq}\left[DEA\right]_{eq}}{\left[DEAH^+\right]_{eq}} = \frac{(m_{H^+}\times\gamma_{H^+})(m_{DEA}\times\gamma_{DEA})}{(m_{DEAH^+}\times\gamma_{DEAH^+})} \quad (30)$$

$$K_2 = \frac{\left[HCO_3^-\right]_{eq}\left[DEA\right]_{eq}}{\left[DEACOO^-\right]_{eq}\left[H_2O\right]_{eq}} = \frac{(m_{HCO_3^-}\times\gamma_{HCO_3^-})(m_{DEA}\times\gamma_{DEA})}{(m_{DEACOO^-}\times\gamma_{DEACOO^-})(\alpha_{H_2O})} \quad (31)$$

$$K_3 = \frac{\left[H^+\right]_{eq}\left[HCO_3^-\right]_{eq}}{\left[CO_2\right]_{eq}\left[H_2O\right]_{eq}} = \frac{(m_{H^+}\times\gamma_{H^+})(m_{HCO_3^-}\times\gamma_{HCO_3^-})}{(m_{CO_2}\times\gamma_{CO_2})(\alpha_{H_2O})} \quad (32)$$

$$K_4 = \frac{\left[H^+\right]_{eq}\left[CO_3^{2-}\right]_{eq}}{\left[HCO_3^-\right]_{eq}} = \frac{(m_{H^+}\times\gamma_{H^+})(m_{CO_3^{2-}}\times\gamma_{CO_3^{2-}})}{(m_{HCO_3^-}\times\gamma_{HCO_3^-})} \quad (33)$$

$$K_5 = \frac{\left[H^+\right]_{eq}\left[OH^-\right]_{eq}}{\left[H_2O\right]_{eq}} = \frac{(m_{H^+}\times\gamma_{H^+})(m_{OH^-}\times\gamma_{OH^-})}{(\alpha_{H_2O})} \quad (34)$$

Mass and charge balance

The DEA balance:

$$C^0_{DEA} = C_{DEA} + C_{DEAH^+} + C_{DEACOO^-} \quad (35)$$

The CO_2 balance:

$$\alpha m_{DEA} = m_{CO_2} + m_{HCO_3^-} + m_{CO_3^{2-}} \quad (36)$$

The charge balance:

$$C_{H^+} + C_{DEAH^+} = C_{CO_3^{2-}} + C_{HCO_3^-} + C_{OH^-} + C_{DEACOO^-} \quad (37)$$

Activity coefficient calculation

To calculate activity coefficients for molecular and ionic species, excess Gibbs energy from the modified Pitzer model is used in the electrolyte solution as follows [48]:

$$\frac{G_E}{RTn_w Mw} = f_1(I) + \sum_{i\neq w}\sum_{j\neq w} m_i m_j \gamma_{ij}(I) + \sum_{i\neq w}\sum_{j\neq w}\sum_{k\neq w} m_i m_j m_k \tau_{ijk} \quad (38)$$

Where $f_1(I)$ is modified Debye-Huckel term defined in the following [48]:

$$f_1(I) = -A_\phi \left(\frac{4I}{1.2}\right)\ln(1+1.2\sqrt{I}) \quad (39)$$

Where A_ϕ and I are the Debye-Huckel parameter and ionic strength, respectively which calculated by [60]:

$$I = \frac{1}{2}\sum_i m_i z_i^2 \quad (40)$$

$$A_\phi = \frac{1}{3}(2\pi N_A \rho_{mix})^{1/2}\left(\frac{e^2}{4\pi\varepsilon_0 Di_{mix} BT}\right)^{3/2} \quad (41)$$

Where m_i and z_i are the molality and charge of component i into the solution, respectively. N_A is the Avogadro's number (6.02205×10^{23} mol^{-1}),ρ_W is the density of water, e is the electron charge (1.6021910^{-19} C), ε_0 is the permittivity of the free space (8.854187×10^{-12}F/m), B is Boltzman constant (1.38065×10^{-23} J/K) and T is the process temperature.ρ_{mix} and Di_{mix} are the mixed solvent density and dielectric constant determined as follow [61]:

$$Di_{mix} = \sum_i v_i D_i \quad (42)$$

$$\rho_{mix} = \left(\sum_i \frac{w_i}{\rho_i}\right)^{-1} \quad (43)$$

Where v_i and w_i are the volume and weight fractions of solvent into the absorbent solution. The density and dielectric are constants of the pure solvent used in the current study presented in Tables 2 and 3.

The ionic strength is dependent on to second Viral coefficient, i.e. λ_{ij} term, defined in the following [48]:

$$\lambda_{ij}(I) = \beta_{ij}^{(0)} + \beta_{ij}^{(1)}\left[(2/x^2)(1-(1+x)e^{-x})\right] \quad (44)$$

$$x = 2(I)^{1/2} \quad (45)$$

B_{ij} is the binary interaction described as the interaction parameters between the different ionic and molecular species in the system, is a function of temperature expressed below:

$$B_{ij}^{(0)} \text{ or } B_{ij}^{(1)} = a_{ij} + b_{ij}T \quad (46)$$

Where a and b are constants for every two species' interactions into the solution illustrated in Table 4.

Due to low concentrations of some species such as OH^-, H^+, and CO_3^{2-}, the interactions between them and other species were neglected to calculate the activity coefficient in the current study as considered in the literature. The activity coefficient of components and water are computed in the following [60]:

$$\ln\gamma_i^{*,m} = -A_\phi z_i^2\left(\frac{\sqrt{I}}{1+1.2\sqrt{I}} + \frac{2}{1.2}\ln(1+1.2\sqrt{I})\right) + 2\sum_{j\neq w} m_j\lambda_{ij}(I) - z_i^2\sum_{j\neq w}\sum_{k\neq w} m_j m_k \frac{\beta_{jk}^{(1)}}{Ix^2}\left[1-(1+x+\frac{x^2}{2})e^{-x}\right] + 3\sum_{j\neq w}\sum_{k\neq w} m_j m_k \tau_{ijk} \quad (47)$$

$$\ln\alpha_{H_2O} = Mw\left(2A_\phi\frac{I^{1.5}}{I+1.2\sqrt{I}} - \sum_{i\neq w}\sum_{j\neq w} m_i m_j(\beta_{ij}^{(0)} + \beta_{ij}^{(1)}e^{-x})\right) - Mw\left(2\sum_{i\neq w}\sum_{j\neq w}\sum_{k\neq w} m_i m_j m_k \tau_{ijk} + \sum_{i\neq w} m_i\right) \quad (48)$$

Where γ_i and α_{H2O} are the activity coefficient of component i and water into the solution. τ is the interaction between three components into the solution that assumed zero in this system.

Solution Strategy

In the modeling of the DEA+H_2O+CO_2 system, eight spices concentrations in the liquid bulk such as DEA, $DEAH^+$, CO_3^{2-}, CO_2, OH^-, H^+, HCO_3^- and $DEACOO^-$ are unknown. These concentrations can be obtained by solving five equilibrium chemical constants, two mass balances, and one charge balance equation, simultaneously. The modeling solution algorithm is depicted in Fig. 2.

Table 2: Density of the pure solvents in the DEA+CO_2+H_2O system.

Solvent	Mw	g/mL)(d	Temperature range (K)	Reference
H_2O	18.02	$\rho = 0.999382 + 0.00007208T - 7.28491\times10^{-6}T^2 + 2.65177\times10^{-8}T^3$	303.15-348.15	[61]
DEA	105.137	$\rho = 1.03526 - 7.6277\times10^{-4}T - 0.08351\times10^{-7}T^2$	303.15-403.15	[62]

Table 3: Dielectric constant of the pure solvents in the DEA+CO2+H2O system.

Component	a	b	Reference
$D = a_i + \frac{b_i}{T}\left(\frac{1}{T} - \frac{1}{298.15}\right)$			
H_2O	78.65	31989	[61]
DEA	25.42	3448275	[62]

Table 4: Species binary interaction (β) in the DEA+CO2+H2O system[53].

Ion/molecule interactions (L/mol)	a_{ij} (L/mol)	b_{ij} (L.K/mol)
$\beta^{(0)}_{DEAH^+-DEA}$	0.801×10^{-3}	-0.150×10^{-3}
$\beta^{(0)}_{DEAH^+-CO_2}$	0.398	-0.199×10^{-8}
$\beta^{(0)}_{DEAH^+-DEACOO^-}$	4.700	-0.116×10^{-1}
$\beta^{(0)}_{DEAH^+-HCO_3^-}$	0.377	-0.678×10^{-6}
$\beta^{(0)}_{DEA-DEA}$	0.703	-0.316×10^{-7}
$\beta^{(0)}_{DEA-CO_2}$	0.805×10^{-5}	-0.130×10^{-6}
$\beta^{(0)}_{DEA-DEACOO^-}$	1.919	-0.491×10^{-2}
$\beta^{(0)}_{DEA-HCO_3^-}$	4.521	-0.129×10^{-1}
$\beta^{(0)}_{CO_2-DEACOO^-}$	0.184×10^{-5}	-0.651×10^{-7}
$\beta^{(0)}_{CO_2-HCO_3^-}$	0.661×10^{-3}	0.679×10^{-3}

RESULTS AND DISCUSSION

DEA solution

Stirrer speed effects on CO_2 loading

As stated in the previous sections, the stirrer speed can affect absorption performance. The DEA concentrations of 0.5 and 1.5 M are investigated at different stirrer speeds. Other operating conditions, i.e. the temperature and pressure are customized at 298 K and 5 bar, respectively. The variation of CO_2 loading versus time is depicted in Fig. 3 under various stirrer speeds. The effects of stirrer speed on equilibrium CO_2 loading are also presented in Fig. 4 for two different DEA concentrations. As shown, by increasing the stirrer speed, the CO_2 loading is increased independent of the DEA concentrations. The equilibrium CO_2 loading was 0.73 and 0.42 for the DEA concentration of 0.5 and 1.5 M, respectively. The kinetic measurement and rate of reactions can be influenced by the stirrer speed due to variation in the gas-liquid surface. During stirring, this hypothesis characterizes the renewal of the gas liquid on the interface based on Danckwerts theory. The rate of reaction and the mass transfer do not change at very low velocities because the speed is not enough to renew the liquid surface. However, at too high velocities, the turbulences on the surface cause a non-stable gas-liquid surface and mass transfer area at the interface. By increasing the stirrer speed from zero to 300 rpm, the maximum value for CO_2 loading is increased about 49% and 65% for DEA concentrations of 0.5 and 1.5 M,

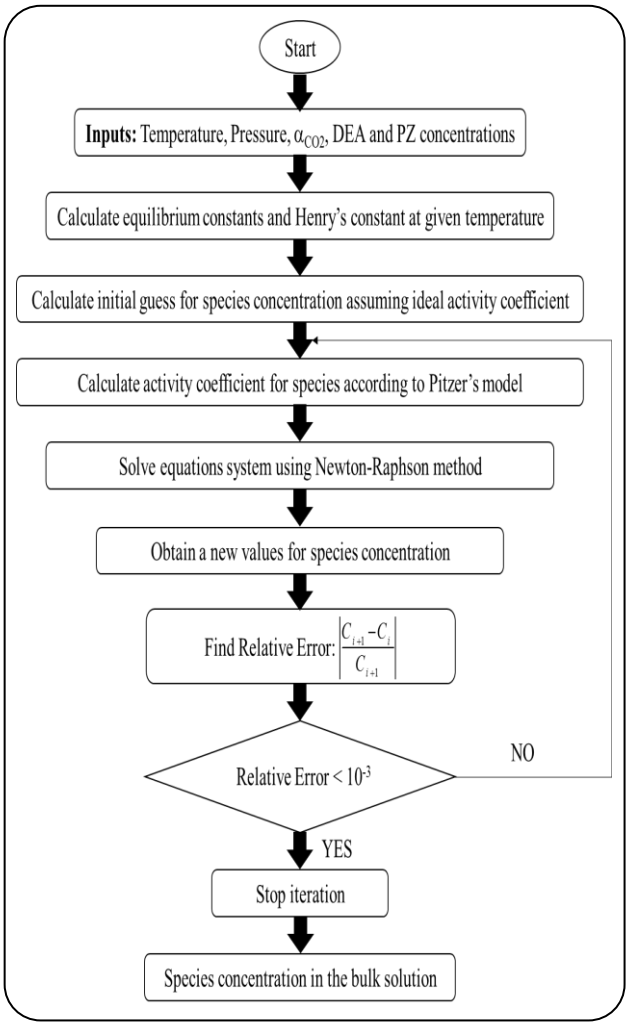

Fig. 2: Solution algorithm of the current modeling.

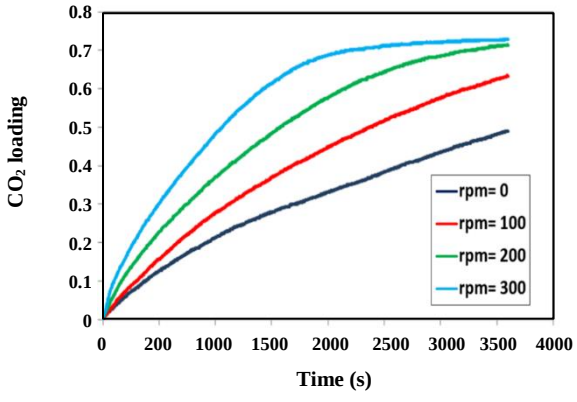

Fig. 3: CO_2 loading vs. time under various stirrer speeds at the DEA concentration of 0.5 M, the temperature of 298 K, and pressure of 5 bar.

respectively. As a result, the effects of stirrer speed on CO_2 loading are enhanced by increasing the absorbent concentration.

Stirrer speed effects on mass transfer flux

The effects of stirrer speed on the mass transfer flux variation are depicted in Fig. 5 at a DEA concentration of 0.5 M. An increase in the stirrer speed causes a change in the mass transfer coefficient, rate of reactions, and process driving force and consequently causes a decrease in the mass transfer flux. As depicted, at initial times and high stirrer speeds, the mass transfer flux is increased significantly. The initial mass transfer flux for 300 rpm relative to 0 rpm is raised 3.5 times at the DEA concentrations of 0.5 M. But at the steady-state and the equilibrium conditions, the mass transfer fluxes are tended to finite values for all speeds. At the equilibrium state, the mass transfer flux values were lower for 300 rpm relative to lower stirrer speeds for both DEA concentrations. This is due to high speeds effects on the mass transfer variations which cause the process equilibrium conditions to be longer and the mass transfer fluxes decrease more than lower speeds during the time. The stirrer speed effect on the mass transfer values at a processing time of 1000s is depicted in Fig. 6 for two DEA concentrations of 0.5 and 1.5 M. The mass transfer flux variations vs. CO_2 loading at different stirrer speeds for the DEA concentration of 1.5 M are also demonstrated in Fig. 7. As time elapses, by increasing the CO_2 loading, the mass transfer fluxes are decreased for all speeds.

Temperature effects

By increasing the temperature, the absorption capacity, solution viscosity, and CO_2 solubility decrease. The effects of temperature on the CO_2 loading are displayed in Fig. 8. Other operating conditions are fixed in this case in which the DEA concentration, initial process pressure, and stirrer speed were 0.5 M, 5 bar, and 100 rpm, respectively. Also, the temperature effects on the equilibrium CO_2 loading are presented in Fig. 9. It was found that by increasing the temperature, the equilibrium loading is decreased about 12% for 45 °C and 19% for 65 °C relative to 25 °C. The mass transfer flux under various temperatures is also represented in Fig. 10. As shown, an increase in the temperature causes enhancement and a reduction in the mass transfer flux at the initial times and equilibrium state,

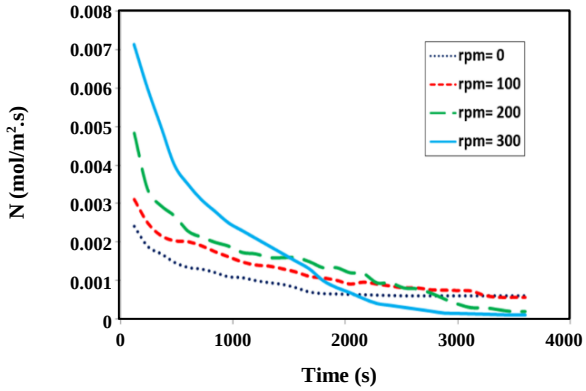

Fig. 4: Mass transfer flux vs. time under various stirrer speeds at the DEA concentrations of 0.5 M, the temperature of 298 K, and pressure of 5 bar.

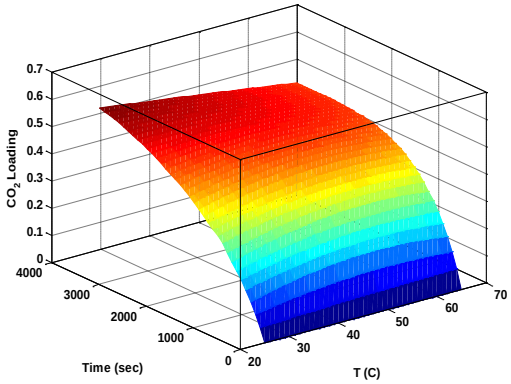

Fig. 7: CO_2 loading variation vs. time under various temperatures and the DEA concentration of 0.5 M, pressure of 5 bar, and stirrer speed of 300 rpm.

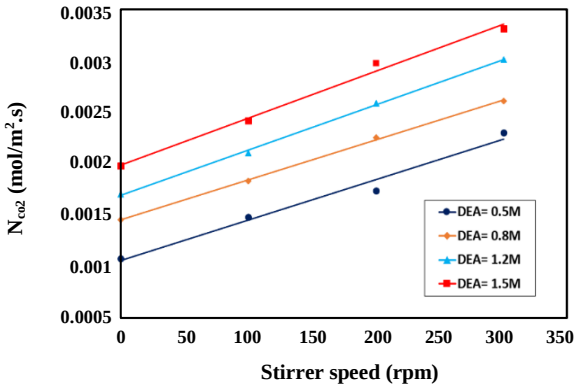

Fig. 5: Effects of stirrer speed on the mass transfer flux under various DEA concentrations and temperature of 298 K, the pressure of 5 bar.

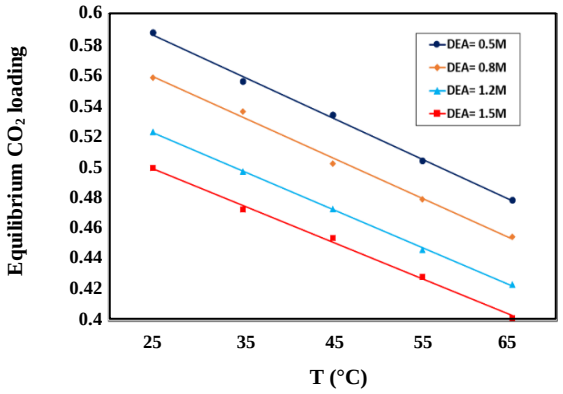

Fig. 8: Effects of temperature on the equilibrium CO_2 loading under various DEA concentrations and the pressure of 5bar and stirrer speed of 300 rpm.

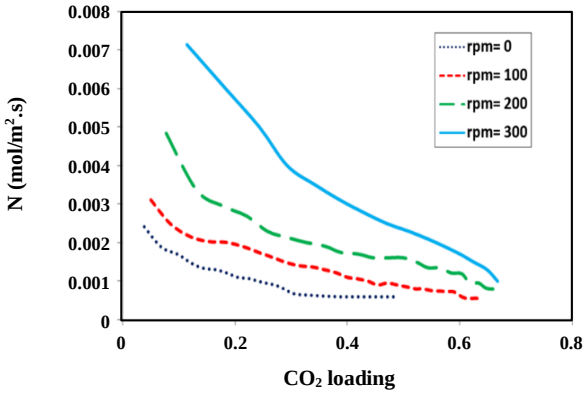

Fig. 6: The mass transfer flux variation vs. CO_2 loading under various stirrer speeds and the DEA concentration of 1.5 M, the temperature of 25 ℃ and pressure of 5 bar.

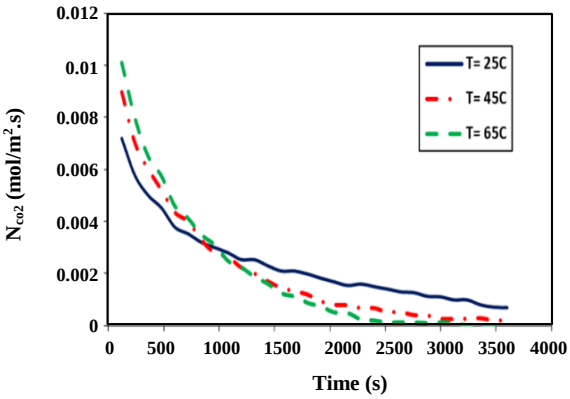

Fig. 9: Effects of temperature on mass transfer flux variation vs. time at the DEA concentration of 0.5 M, pressure of 5 bar, and stirrer speed of 300 rpm.

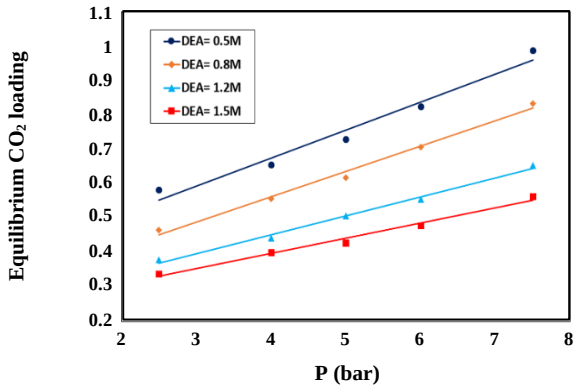

Fig. 10: Effects of pressure on equilibrium CO_2 loading under various DEA concentrations at temperature of 25 ℃ and stirrer speed of 300 rpm.

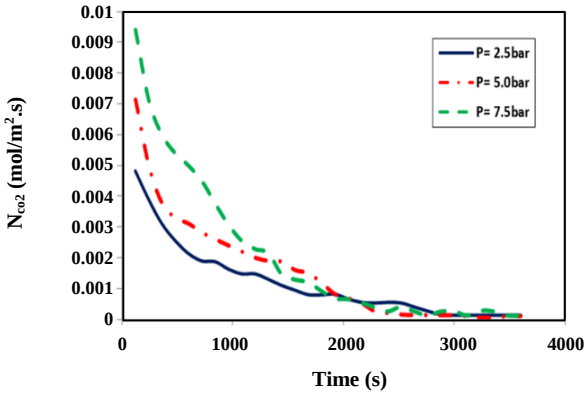

Fig. 11: Effects of pressure on mass transfer flux variation vs. time at DEA concentration of 0.5 M, temperature of 25 ℃ and stirrer speed of 300 rpm.

respectively. It is due to its lower rate of reactions caused lower absorption at initial times and required a longer time to be steady at the equilibrium state for lower temperatures.

Pressure effects

The pressure impacts on the equilibrium CO_2 loading are depicted in Fig. 11. As expected, by increasing the initial process pressure, the mole of CO_2 absorbed at a fixed number of absorbent moles is increased. By enhancing the pressure from 2.5 to 7.5 bar, the equilibrium CO_2 loading is increased 69%. The effects of this operating condition on the mass transfer flux are also investigated in Fig. 12. An increase in the pressure causes higher mass transfer fluxes at initial times significantly but at the final process times, its effects on the mass flux are declined.

Concentration effects

As expected from Eq. 22, by increasing the absorbent concentration, the number of absorbents in the denominator of this equation increases at a much higher rate compared to the moles of CO_2 absorbed, thus increasing the absorbent moles overcomes the increment of the CO_2 absorbed moles leads to a decrease in the CO_2 loading. The variation of CO_2 loading versus time and the DEA concentration is depicted as a 3D plot in Fig. 13. As shown, by increasing the DEA concentration, the initial CO_2 loadings and slope of its variation versus time are decreased. The effects of the DEA concentrations on the equilibrium CO_2 loading are also shown in Fig. 14. As can be observed, the DEA concentration has a reverse relation with the equilibrium CO_2 loading.

Molecular and ionic species concentration

As mentioned, the combination of the Pitzer model, mass balance, charge balance, and chemical reactions equilibrium equations are used to calculate the concentration of ions and molecules into the aqueous DEA solution. The concentration of the components in the DEA+CO_2+H_2O system is predicted and showed in Figs. 15 and 16 for two different stirrer speeds. Fig. 14 predicted the species concentrations at a stirrer speed of 0 rpm and Fig. 15 at 300 rpm. By increasing the stirrer speed, the equilibrium concentration of the DEA molecule is decreased 40% and the equilibrium concentration of $DEAH^+$ and HCO_3^- ions are increased by 73% and 85%, respectively. The concentrations of the other ions and molecules are also increased by increasing speed. Since the OH^- and H^+ concentrations are not affected by the stirrer speed significantly and have very low values, the concentration of these ions is not reported.

Equilibrium loading and absorption rate

The CO_2 loading and absorption rate are presented at the equilibrium state and various stirrer speeds after 1h in Table 5. As stated in sections 6.1.1 and 6.1.4, the CO_2 loading increases by enhancing the stirrer speed and decreasing the DEA concentration. Also from the results, it can be deduced that an increase in the DEA concentrations and stirrer speed caused an increment in the absorption rate. The minimum value for the absorption rate was calculated 27.83% for the DEA concentration of 0.5 M and the stirrer speed of 0 rpm, and the maximum value was 72.61% for 1.5 M and 300 rpm.

Table 5: CO_2 loading and absorption rate in the DEA+CO_2+H_2O system after 3600 seconds.

Speed (rpm)	0		100		200		300	
DEA (M)	α	R (%)	α	R (%)	α	R (%)	α	R (%)
0.5	0.490	27.83	0.633	35.89	0.713	40.64	0.730	41.48
1.0	0.319	36.24	0.395	44.90	0.497	56.38	0.573	65.03
1.5	0.260	44.42	0.308	52.60	0.366	62.23	0.425	72.61

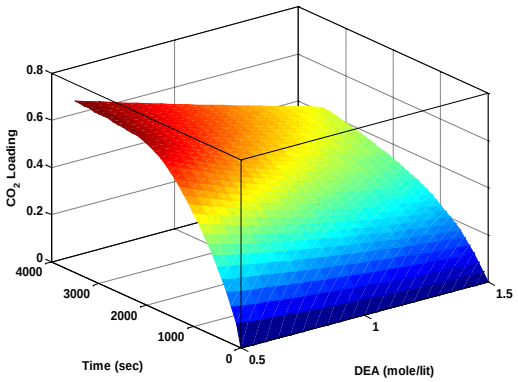

Fig. 12: Mass transfer flux vs. time and DEA concentration at the pressure of 5 bar, the temperature of 25 ℃ and stirrer speed of 300 rpm.

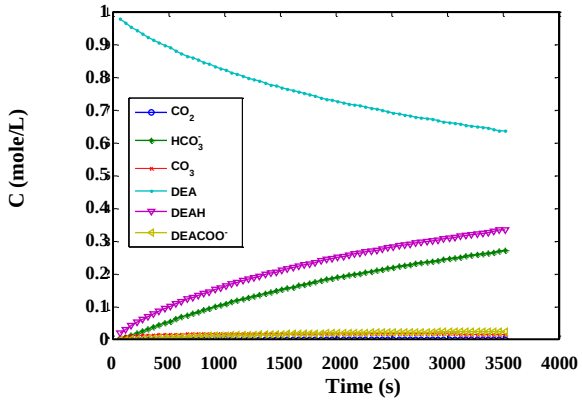

Fig. 14: Ionic and molecular species concentrations vs. time in the DEA electrolyte system at the stirrer speed of 0rpm, DEA concentration of 1 M, the pressure of 5 bar, and temperature of 25 ℃.

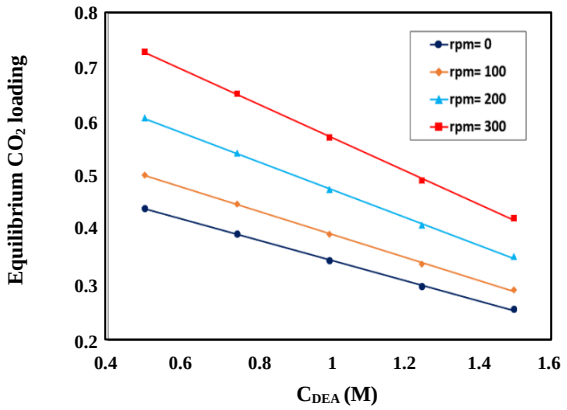

Fig. 13: Effects of the DEA concentration on the equilibrium CO_2 loading under various DEA concentrations and the pressure of 5 bar and temperature of 25 ℃.

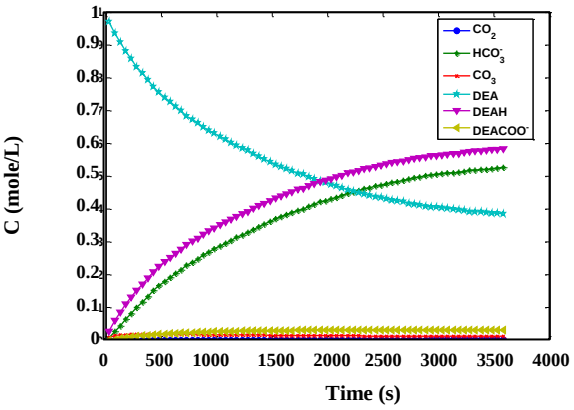

Fig. 15: Ionic and molecular species concentrations vs. time in the DEA electrolyte system at the stirrer speed of 300 rpm, DEA concentration of 1 M, the pressure of 5 bar, the temperature of 25 ℃.

DEA+PZ blend solution

Effects of concentration on CO_2 loading

The effects of absorbent concentration on the CO_2 loading in the PZ+DEA+CO_2+H_2O system are investigated in Fig. 16. As shown, by increasing the PZ concentration and decreasing the DEA concentration, the CO_2 loading increases. The maximum value for CO_2 loading is obtained with the PZ concentration of 0.5 M and the DEA concentration of 0 M. The values of equilibrium CO_2 loading are obtained 0.73, 0.84, 0.87, and 0.94 when the absorbent was only 0.5 M DEA, 0.3 M DEA, and 0.2 M PZ, 0.2 M DEA, and 0.3 M PZ, and only 0.5 M PZ,

Table 6: Equilibrium CO_2 loading and pressure in the DEA+PZ+CO_2+H_2O system after 3600 seconds.

DEA	0.0	0.1	0.2	0.3	0.4	0.5
PZ	0.5	0.4	0.3	0.2	0.1	0.0
Equilibrium CO_2 Loading	0.9458	0.9257	0.8760	0.8462	0.8250	0.7297
Equilibrium Pressure	2.401	2.366	2.621	2.626	2.630	2.927

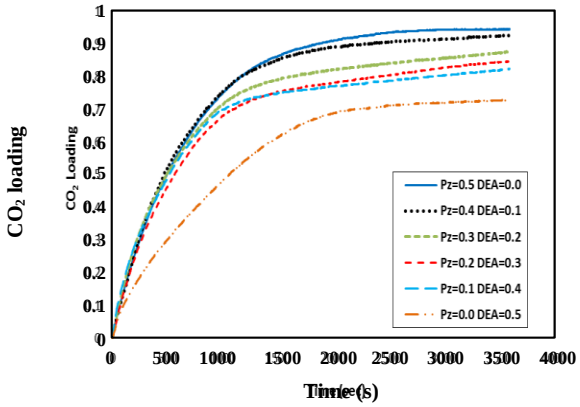

Fig. 16: Effects of the DEA and PZ concentrations on the CO_2 loading in the DEA+PZ+CO_2+H_2O system at the DEA concentration of 1 M, the pressure of 5 bar, the temperature of 25 ℃, and stirrer speed of 300 rpm.

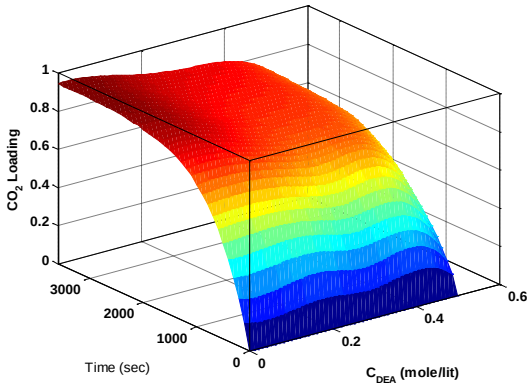

Fig. 17: CO_2 loading variations vs. DEA concentration in the DEA+PZ+CO_2+H_2O system at the PZ concentration of 0.5 M, the pressure of 5 bar, the temperature of 25 ℃, and stirrer speed of 300 rpm.

respectively as stated in Table 7. It can be concluded that only using PZ solution as the absorbent is more effective than the PZ+DEA+H_2O blend and only DEA solution. The effects of DEA concentration on the DEA+PZ+H_2O blend solution performance and the CO_2 loading at a fixed PZ concentration of 0.5 M are shown in Fig. 17. By increasing the DEA concentration at the fixed PZ concentration, the CO_2 loading is decreased.

Effects of concentration on equilibrium loading and pressure

The equilibrium CO_2 loading and pressure are represented in Table 6 under various PZ and DEA concentrations into the DEA+PZ+H_2O blend solution. As mentioned in the previous section, the equilibrium loading is decreased by increasing the DEA concentration. As also resulted, at the same initial pressures, the equilibrium pressure is increased 22% by increasing the DEA concentration from 0 to 0.5 M.

CONCLUSIONS

The CO_2 capture by the absorption process is studied using the DEA and DEA+PZ+H_2O blend solution in the current study. In these processes, various variables such as CO_2 loading, absorption rate, and mass transfer rate are very influential. The effects of various operating parameters on these variables are also examined. The experiments are performed at operational conditions of the temperature range of 25-65 ℃, pressure range of 1.5-6.5 bar, and DEA concentration of 0-1.5 M, PZ concentration of 0-0.5 M and stirrer speeds of 0-300 rpm. The species concentrations into the DEA solution are predicted based on solving the Pitzer model, mass and charge equations simultaneously. Based on the experimental results into the DEA solution, by increasing the stirrer speed from 0 to 300 rpm, the mass transfer flux increased, and also the maximum value of CO_2 loading is increased by 65% for the DEA concentration of 1.5 M, which this increment was more than the lower DEA concentration of 0.5 M. The maximum value for loading is decreased by increasing the process temperature and reducing the initial pressure. With an enhancement in the initial pressure from 2.5 to 7.5 bar, the maximum loading is also enhanced by 69%. Due to enhancing the number of absorbent moles by increasing the DEA concentration and low absorption capacity for the DEA solution, the CO_2 loading is decreased. The predicted

concentrations in the modeling showed that by increasing the stirrer speeds, the equilibrium concentration of the DEA molecule is decreased but the concentrations of other ionic and molecular species are increased. Adding the PZ to the absorbent solution caused a more absorption rate and CO_2 loading than the DEA solution. The equilibrium CO_2 loadings and pressures are obtained 0.94 and 0.73 for only PZ and DEA solutions, respectively.

Nomenclature

P	Pressure, bar
T	Temperature, K
R	Universal gas constant
C	Concentration, mol/mL
G	Gibbs energy
E	Enhancement factor
A_ϕ	Debye-Huckel parameter
a, b, c, d, e	Constants
n	Number of moles
m	Molality, mol/kg
Mw	Molecular weight
M	Film parameter
ν	Stoichiometric coefficient
v	Volume fraction, %
w	Weight fraction, %
k	Mass transfer coefficient, m^2/s
K	Chemical equilibrium constant
N	Mass transfer flux, mol / m^2.s
H	Henry's constant, MPa.kg,mol
B	Botlzman constant
I	Ionic strength
N_A	Avogadro's number, mol
e	Electron charge, C
z	Charge of ion
D	Diffusion coefficient
Di	Dielectric constant

Greek

ρ	Density, g/mL
α_{CO2}	CO_2 loading in liquid phase
α_{H2O}	Water activity
β	Binary interaction parameters
τ	Tertiary interaction parameters
γ	Activity coefficient
ε	Permittivity, F/m

Subscript

i, j, k	Numerators
i0	Initial
f	Final
b	Bulk
int	Interface
l	Liquid
g	Gas
G	Overall resistance in the gas phase
mix	Mixture

Received : Oct. 14, 2019 ; Accepted : Feb. 17, 2020

REFERENCES

[1] Fu D., Wang L., Mi C., Zhang P., Absorption Capacity and Viscosity for CO_2 Capture Process Using High Concentrated PZ-DEAE Aqueous Solution, *The Journal of Chemical Thermodynamics*, **101**: 123-129 (2016).

[2] Kazemi S., Ghaemi A., Tahvildari K., Chemical Absorption of Carbon Dioxide into Aqueous Piperazine Solutions Using a Stirred Reactor, *Iranian Journal of Chemistry and Chemical Engineering (IJCCE)*,**39(4)**: 253-267 (2019).

[3] Wang M., Lawal A., Stephenson P., Sidders J., Ramshaw C., "Post-Combustion CO_2 Capture with Chemical Absorption: A State-of-the-Art Review, *Chemical Engineering Research and Design*, **89(9)**: 1609-1624 (2011).

[4] Ling H., Liu S., Gao H., Liang Z., Effect of Heat-Stable Salts on Absorption/Desorption Performance of Aqueous Monoethanolamine (MEA) Solution During Carbon Dioxide Capture Process, *Separation & Purification Technology*, **212**: 822-833 (2019).

[5] Karbalaei Mohammad N., Ghaemi A., Tahvildari K., Experimental Investigation and Modeling of CO_2 Adsorption Using Modified Activated Carbon, *Iranian Journal of Chemistry and Chemical Engineering (IJCCE)*, **39(1)**: 177-192 (2020).

[6] Saeidi M., Ghaemi A., Tahvildari K., CO_2 Capture Exploration on Potassium Hydroxide Employing Response Surface Methodology, Isotherm and Kinetic Models, *Iranian Journal of Chemistry and Chemical Engineering (IJCCE)*, **39(5):** 255-267 (2020).

[7] Pashaei H., Ghaemi A., Nasiri M., Modeling and Experimental Study on the Solubility and Mass Transfer of CO_2 into Aqueous DEA Solution Using a Stirrer Bubble Column, *RSC Advances*, **6**: 108075-108092 (2016).

[8] Pashaei H., Zarandi M.N., Ghaemi A., Experimental Study and Modeling of CO_2 Absorption into Diethanolamine Solutions Using Stirrer Bubble Column, *Chemical Engineering Research and Design*, **121**: 32-43 (2017).

[9] Adeosun A., El Hadri N., Goetheer E., Abu-Zahra M. R., Absorption of CO_2 by Amine Blends Solution: An Experimental Evaluation, *International Journal of Engineering And Science*, **3**: 12-23 (2013).

[10] Ghaemi A., Shahhosseini Sh., Ghannadi Maragheh M., Experimental Investigation of Reactive Absorption of Ammonia and Carbon Dioxide by Carbonated Ammonia Solution, *Iranian Journal of Chemistry and Chemical Engineering (IJCCE)*, **30(2)**: 43-50., (2011).

[11] Bui M., Gunawan I., Verheyen V., Feron P., Meuleman E., Adeloju S., Dynamic Modelling and Optimisation of Flexible Operation in Post-Combustion CO_2 Capture Plants—A Review, *Computers Chemical Engineering*, **61**: 245-265, (2014).

[12] Wai S.K., Nwaoha C., Saiwan C., Idem R., Supap T., Absorption Heat, Solubility, Absorption and Desorption Rates, Cyclic Capacity, Heat Duty, and Absorption Kinetic Modeling of AMP–DETA Blend for Post–Combustion CO_2 Capture, *Separation & Purification Technology*, **194**: 89-95 (2018).

[13] Ghaemi A., Jafari Z., Etemad E., Prediction of CO_2 Mass Transfer Flux in Aqueous Amine Solutions Using Artificial Neural Networks, *Iranian Journal of Chemistry and Chemical Engineering (IJCCE)*, **39(4)**: 269-280 (2020).

[14] Dashti A., Raji M., Razmi A., Rezaei N., Zendehboudi S., Asghari M., Efficient Hybrid Modeling of CO_2 Absorption in Aqueous Solution of Piperazine: Applications to Energy and Environment, *Chemical Engineering Research and Design*, **144**: 405-417 (2019).

[15] Lee H. S., Lee N. R., Yang D. R., A New Method of Amine Solvent Recovery with Acid Addition for Energy Reduction in the CO_2 Absorption Process, *Chemical Engineering Research and Design*, **91(12)**: 2630-2638 (2013).

[16] Muchan P., Narku-Tetteh J., Saiwan C., Idem R., Supap T., Effect of Number of Amine Groups in Aqueous Polyamine Solution on Carbon Dioxide (CO_2) Capture Activities, *Separation & Purification Technology*, **184**: 128-134 (2017).

[17] Shi H., Huang M., Huang Y., Cui M., Idem R., CO_2 Absorption Efficiency of Various MEA-DEA Blend with Aid of $CaCO_3$ and $MgCO_3$ in a Batch and Semi-Batch Processes, *Separation & Purification Technology*, **220**: 102-113 (2019).

[18] Moioli S., Pellegrini L.A., Describing Physical Properties of CO_2 Unloaded and Loaded MDEA+ PZ Solutions, *Chemical Engineering Research and Design*, **138**: 116-124 (2018).

[19] Norouzbahari S., Shahhosseini S., Ghaemi A., Chemical Absorption of CO_2 into an Aqueous Piperazine (PZ) Solution: Development and Validation of a Rigorous Dynamic Rate-Based Model, *RSC Advances*, **6**: 40017-40032 (2016).

[20] Pashaei H., Ghaemi A., Nasiri M., Experimental Investigation of CO_2 Removal Using Piperazine Solution in a Stirrer Bubble Column, *International Journal of Greenhouse Gas Control*, **63**: 226-240, (2017).

[21] Norouzbahari S., Shahhosseini S., Ghaemi A., Modeling of CO_2 Loading in Aqueous Solutions of Piperazine: Application of an Enhanced Artificial Neural Network Algorithm, *Journal of Natural Gas Science and Engineering*, **24**:18-25 (2015).

[22] Norouzbahari S., Shahhosseini S., Ghaemi A., CO_2 Chemical Absorption Into Aqueous Solutions of Piperazine: Modeling of Kinetics and Mass Transfer Rate, *Journal of Natural Gas Science Engineering*, **26**: 1059-1067 (2015).

[23] Norouzbahari S., Shahhosseini S., Ghaemi A., Chemical Absorption of CO_2 into an Aqueous Piperazine (PZ) Solution: Development and Validation of a Rigorous Dynamic Rate-Based Model, *RSC Advances*, **6**: 40017-40032 (2016).

[24] Heydarifard M., Pashaei H., Ghaemi A., Nasiri M., Reactive Absorption of CO_2 into Piperazine Aqueous Solution in a Stirrer Bubble Column: Modeling and Experimental, *International Journal of Greenhouse Gas Control*, **79**: 91-116 (2018).

[25] Moioli S., Pellegrini L.A., Physical Properties of PZ Solution Used as a Solvent for CO_2 Removal, *Chemical Engineering Research and Design*, **93**: 720-726 (2015).

[26] Fashi F., Ghaemi A., Moradi P., Piperazine-Modified Activated Alumina as a Novel Promising Candidate for CO_2 Capture: Experimental and Modeling, *Greenhouse Gases: Science and Technology*, **9**: 37-51 (2019).

[27] Mirzaei F., Ghaemi A., An Experimental Correlation for Mass Transfer Flux of CO_2 Reactive Absorption into Aqueous MEA-PZ Blended Solution, *Asia-Pacific Journal of Chemical Engineering*, **13(6)**: e2250 (2018.)

[28] Godini H. R., Mowla D., Selectivity Study of H_2S and CO_2 Absorptionfrom Gaseous Mixtures by MEA in Packed Beds, *Chemical Engineering Research and Design*, **86(4)**: 401-409 (2008).

[29] Zhang Z., Chen F., Rezakazemi M., Zhang W., Lu C., Chang H., Quan X., Modeling of a CO_2-Piperazine-Membrane Absorption System, *Chemical Engineering Research and Design*, **131**: 375-384 (2018).

[30] Zhu D., Fang M., Lv Z., Wang Z., Luo Z., Selection of Blended Solvents for CO_2 Absorption from Coal-Fired Flue Gas. Part 1: Monoethanolamine (MEA)-Based Solvents" *Energy & Fuels*, **26(1)**: 147-153 (2011).

[31] Ramazani R., Mazinani S., Hafizi A., Jahanmiri A., Equilibrium Solubility of Carbon Dioxide in Aqueous Blend of Monoethanolamine (MEA) and 2-1-Piperazinyl-Ethylamine (PZEA) Solutions: Experimental and Optimization Study, *Process Safety and Environmental Protection*, **98**: 325-332 (2015).

[32] Nwaoha C., Saiwan C., Tontiwachwuthikul P., Supap T., Rongwong W., Idem R., Al-Marri M.J., Benamor A., Carbon Dioxide (CO_2) Capture: Absorption-Desorption Capabilities of 2-Amino-2-Methyl-1-Propanol (AMP), Piperazine (PZ) and Monoethanolamine (MEA) Tri-Solvent Blends, *Journal of Natural Gas Science Engineering*, **33**: 742-750 (2016).

[33] Hairul N., Shariff A., Tay W., Mortel A., Lau K., Tan L., Modelling of High Pressure CO_2 Absorption Using PZ+ AMP Blended Solution in a Packed Absorption Column, *Separation and Purification Technology*, **165**: 179-189 (2016).

[34] Wang T., Liu F., Ge K., Fang M., Reaction Kinetics of Carbon Dioxide Absorption in Aqueous Solutions of Piperazine, N-(2-Aminoethyl) Ethanolamine and Their Blends, *Chemical Engineering Journal*, **314**: 123-131 (2017).

[35] Du Y., Wang Y., Rochelle G.T., Thermal degradation of Novel Piperazine-Based Amine Blends for CO_2 Capture, *International Journal of Greenhouse Gas Control*, **49:**239-249 (2016).

[36] Das B., Deogam B., Mandal B., Absorption of CO_2 into novel Aqueous bis (3-aminopropyl) Amine and Enhancement of CO_2 Absorption into its Blends with N-methyldiethanolamine, *International Journal of Greenhouse Gas Control*, **60**: 172-185 (2017).

[37] Zhang P., Xu R., Li H., Gao H., Liang Z., Mass Transfer Performance for CO_2 Absorption into Aqueous Blended DMEA/MEA Solution with Optimized Molar Ratio in a Hollow Fiber membrane Contactor, *Separation and Purification Technology*, **211**: 628-636 (2019).

[38] Zhang T., Yu Y., Zhang Z., An Interactive Chemical Enhancement of CO_2 Capture in the MEA/PZ/AMP/DEA Binary Solutions, *International Journal of Greenhouse Gas Control*, **74**:119-129, (2018).

[39] Saidi M., Process Assessment and Sensitivity Analysis of CO_2 Capture by Aqueous Methyldiethanolamine+ Piperazine Blended Solutions Using Membrane Contactor: Model Development of Kinetics and Mass Transfer Rate, *Separation & Purification Technology*, **204:**185-195 (2018).

[40] Suleman H., Maulud A.S., Man Z., Experimental Measurements and Modeling of Carbon Dioxide Solubility in Aqueous AMP/MDEA and Piperazine/MDEA Blends, *Fluid Phase Equilibria*, **463:**142-148 (2018).

[41] Afkhamipour M., Mofarahi M., Pakzad, C. Lee - P.H., Thermodynamic Modelling of CO_2 Absorption into Aqueous Solutions of 2-diethylaminoethanol, Piperazine, and Blended Diethylaminoethanol with Piperazine, *Fluid Phase Equilibria*, 493: 26-35 (2019).

[42] Hosseini Jenab M., Abedinzadegan Abdi M., Najibi S.H., Vahidi M., Matin N.S., Solubility of Carbon Dioxide in Aqueous Mixtures of N-methyldiethanolamine+ Piperazine+ Sulfolane, *Journal of Chemical Engineering Data*, **50(2)**: 583-586 (2005).

[43] Dey A., Aroonwilas A., CO_2 Absorption into MEA-AMP Blend: Mass Transfer and Absorber Height Index, *Energy Procedia*, **1**(1): 211-215 (2009).

[44] Luo W., Guo D., Zheng J., Gao S., Chen J., CO_2 Absorption Using Biphasic Solvent: Blends of Diethylenetriamine, Sulfolane, and Water, *International Journal of Greenhouse Gas Control*, **53**: 141-148 (2016).

[45] Edali M., Idem R., Aboudheir A., 1D and 2D Absorption-rate/kinetic modeling and simulation of Carbon Dioxide Absorption into Mixed Aqueous Solutions of MDEA and PZ in a Laminar Jet Apparatus, *International Journal of Greenhouse Gas Control*, **4(2):** 143-151 (2010).

[46] Liu J., Wang S., Zhao, B. Qi G., Chen C., Study on Mass Transfer and Kinetics of CO_2 Absorption into Aqueous Ammonia and Piperazine Blended Solutions, *Chemical Engineering Science*, **75**: 298-308 (2012).

[47] Ghaemi A., Torab-Mostaedi M., Maragheh M.G., Shahhosseini S., Kinetics and Absorption Rate of CO_2 into Partially Carbonated Ammonia Solutions, *Chemical Engineering Communications*, **198(10)**: 1169-1181 (2011).

[48] Bougie F., Iliuta M.C., CO_2 Absorption in Aqueous Piperazine Solutions: Experimental Study and Modeling, *Journal of Chemical Engineering Data*, **56(4):** 1547-1554 (2011).

[49] Danckwerts P., Significance of Liquid-Film Coefficients in Gas Absorption, *Industrial Engineering Chemistry*, **43(6)**: 1460-1467 (1951).

[50] Saeidi M., Ghaemi A., Tahvildari K., Derakhshi P., Exploiting Response Surface Methodology (RSM) as a Novel Approach for the Optimization of Carbon Dioxide Adsorption by Dry Sodium Hydroxide, *Journal of the Chinese Chemical Society*, **65(12)**: 1465-1475 (2018).

[51] Kim Y.E., Lim J.A., Jeong S.K., Yoon Y.I., Bae S.T., Nam S.C., Comparison of Carbon Dioxide Absorption in Aqueous MEA, DEA, TEA, and AMP Solutions, *Bulletin of the Korean Chemical Society*, **34(3)**: 783-787 (2013).

[52] Saghafi H., Ghiasi M.M., Mohammadi A.H., Analyzing the Experimental data of CO_2 Equilibrium Absorption in the Aqueous Solution of DEA+ MDEA with Random Forest and Leverage Method, *International Journal of Greenhouse Gas Control*, **63**: 329-337 (2017).

[53] Benamor A., Aroua M., Modeling of CO_2 Solubility and Carbamate Concentration in DEA, MDEA and Their Mixtures Using the Deshmukh–Mather Model, *Fluid Phase Equilibria*, **231(2)**:150-162, 2005.

[54] Perrin D.D., Dissociation Constants of Organic Bases in Aqueous Solution: Supplement 1972". Butterworths, 1972.

[55] Edwards T.J., Newman J., Prausnitz J.M., Thermodynamics of Aqueous Solutions Containing Volatile Weak Electrolytes, *AIChE Journal*, **21(2)**: 248-259, 1975.

[56] Patterson C., Slocum G., Busey R., Mesmer R., Carbonate Equilibria in Hydrothermal Systems: First Ionization of Carbonic Acid in NaCl Media to 300 °C, *Geochimica et Cosmochimica Acta*, **46(9):** 1653-1663 (1982).

[57] Patterson C., Busey R., Mesmer R., Second ionization of Carbonic Acid in NaCl Media to 250 °C, *Journal of Solution Chemistry*, **13(9)**: 647-661 (1984).

[58] Edwards T., Maurer G., Newman J., Prausnitz J., Vapor-Liquid Equilibria in Multicomponent Aqueous Solutions of Volatile Weak Electrolytes, *AIChE Journal*, **24(6)**: 966-976 (1978).

[59] Roberts B.E, Mather A.E., Solubility of CO_2 and H_2S in a Mixed Solvent, *Chemical Engineering Communications*,,**72(1)**: 201-211 (1988).

[60] Bougie F., Iliuta M.C., CO_2 Absorption into Mixed Aqueous Solutions of 2-amino-2-hydroxymethyl-1, 3-Propanediol and Piperazine, *Industrial Engineering Chemistry Research*, **49(3)**:150-1159 (2009).

[61] Qian W.-M., Li Y.-G., Mather A. E., Correlation and Prediction of the Solubility of CO_2 and H_2S in an Aqueous Solution of Methyldiethanolamine and Sulfolane, *Industrial and Engineering Chemistry Research*, **34(7)**: 2545-2550 (1995).

[62] Teng T., Maham Y., Hepler L., Mather A., Measurement and Prediction of the Density of Aqueous Ternary Mixtures of Methyldiethanolamine and Diethanolamine at Temperatures from 25°C to 80°C, *The Canadian Journal of Chemical Engineering*, **72(1):** 125-129 (1994).

[63] Maham Y., Teng T., Hepler L., Mather A., Volumetric Properties of Aqueous Solutions of Monoethanolamine, Mono-and Dimethylethanolamines at Temperatures from 5 to 80° C, *Thermochimica Acta*, **386(2)**: 111-118 (2002).